Chapter 5

MO Knockdown of CapZ Subunits and Confirmation of *sne* Positional Cloning

Chapter 5: MO Knockdown of CapZ Subunits and confirmation of *sne* positional cloning

5.1 Summary

In this chapter antisense morpholino oligonucleotides (MOs) were used to: 1) examine the functions of the various CapZ subunits, 2) determine the extent of CapZα1 function in the *sne* mutant and 3) confirm that the mutation in *capzα1* is the cause of the *sne* mutant phenotype. Unfortunately, MO analysis of CapZα2 function was inconclusive in determining whether it was partially redundant to CapZα1. Interestingly, severe developmental defects, much worse than the *sne* mutant phenotype, were observed from complete ablation of CapZ (either by injection of high doses of capZβ MO or knockdown of both α subunits). These findings indicate that the mutation in *sne* does not completely ablate CapZ function, and suggests that the *sne* mutant is hypomorphic. Western analysis performed to conclusively determine which different transcripts were translated in the *sne* mutant was unsuccessful. Finally, the morphants (that is MO injected embryos) generated from the knockdown of the various CapZ subunits confirm that the *sne* phenotype is caused by a mutation in *capzα1*. Moreover, the CapZα1 morphant phenotype is partially rescued by over expression of *capzα1*-GFP.

5.2 Introduction

Very little is known about the role of CapZ in vertebrate development and only a handful of studies have looked at CapZ in an *in vivo* context. CapZ is able to cap the barbed end of actin filaments that are localized in all cell types. Indeed, actin filaments are involved in many different processes including cell motility, cytokinesis and are integral to the cellular cytoskeleton. It is therefore likely that CapZ plays an important role in controlling actin dynamics early in development, where gastrulation cell movements are critical to embryogenesis. In order to gain a

greater understanding of how CapZ is involved in development, MO knockdowns on one or more of the CapZ subunits were performed. The MOs were also used to investigate the extent of function of the mis-spliced forms of CapZα1 in the *sne* mutants, as well as to determine whether the *sne* mutant phenotype could be replicated by knockdown of CapZα1. Western blotting was performed to identify which transcripts were translated in the mutant and to verify the effectiveness of each MO. Finally, a *capzα1*-GFP fusion construct was generated to confirm the localization of CapZα1 *in vivo* and to rescue a capZα1 morphant with exogenous CapZα1.

5.3 MO knockdown of the CapZ subunits

In the previous chapter antibody staining revealed that the mis-spliced forms of CapZα1 were translated in the mutants. MOs against all the CapZ subunits were therefore used to determine firstly, whether the mutant forms of CapZα1 were functional. Secondly, to confirm that the *sne* phenotype was indeed a result of the mutation in *capzα1*, and finally to ascertain whether CapZα2 could compensate for the loss of CapZα1. MOs that targeted the start site and splice sites of each subunit (*capzα1*, *capzα2* and *capzβ*) were designed to look at the effect of knocking down the zygotic contribution (splice MO) versus the maternal and zygotic contribution (ATG MO). The sequences of all MOs used are listed in Table 1, Chapter 2, and the target sites for the MOs are illustrated in Fig. 5.1. See appendix, Table 4 for the number of experiments performed with each MO.

5.3.1 MO knockdown of CapZα1

Initially, CapZα1 was completely knocked down with an ATG or splice 1 MO to determine whether the *sne* phenotype could be replicated. However, as suspected, the morphant embryos had a more severe phenotype than the *sne* mutant. Injection of capZα1 ATG MO (5ng) resulted in embryos that were developmentally delayed, had smaller brains and eyes, less

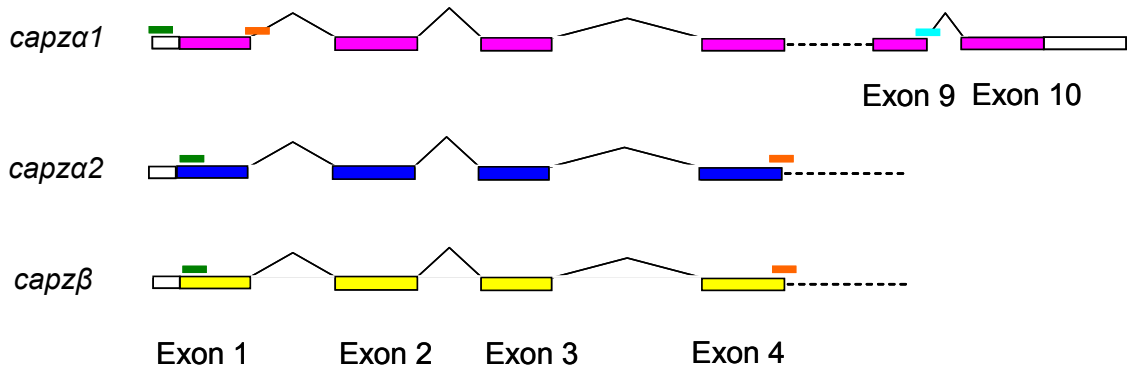

Fig. 5.1. Schematic diagram of MO target sites for *capzα1*, *capα2* and *capzβ*. The green bars represent the target sites for the ATG MOs, the orange bars represent the target site for the splice 1 MOs and the blue bar represents the target site for the MO that phenocopies the mutation in the *sne* mutant (capZα1 splice 2). Blocks that are not coloured are UTRs.

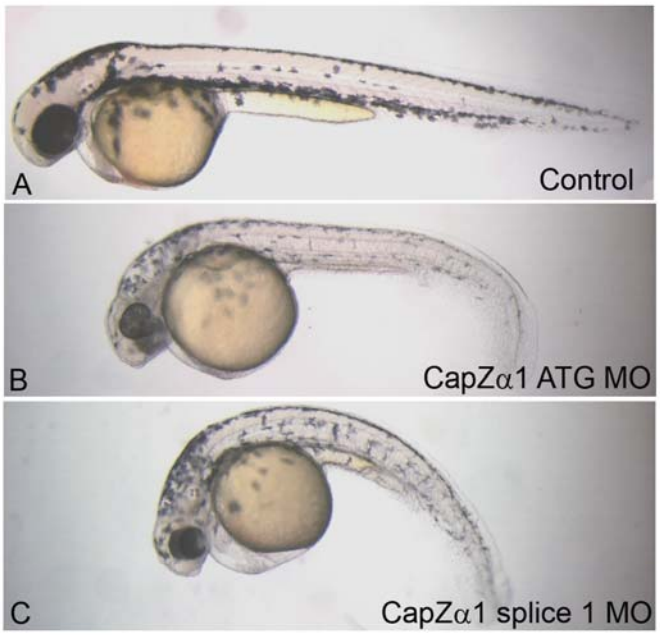

Fig. 5.2. 48 hpf embryos injected with a capZα1 ATG and splice 1 MO. A) Buffer injected control, B) 5ng of capZα1 ATG MO, C) 4ng of capZα1 splice 1 MO.

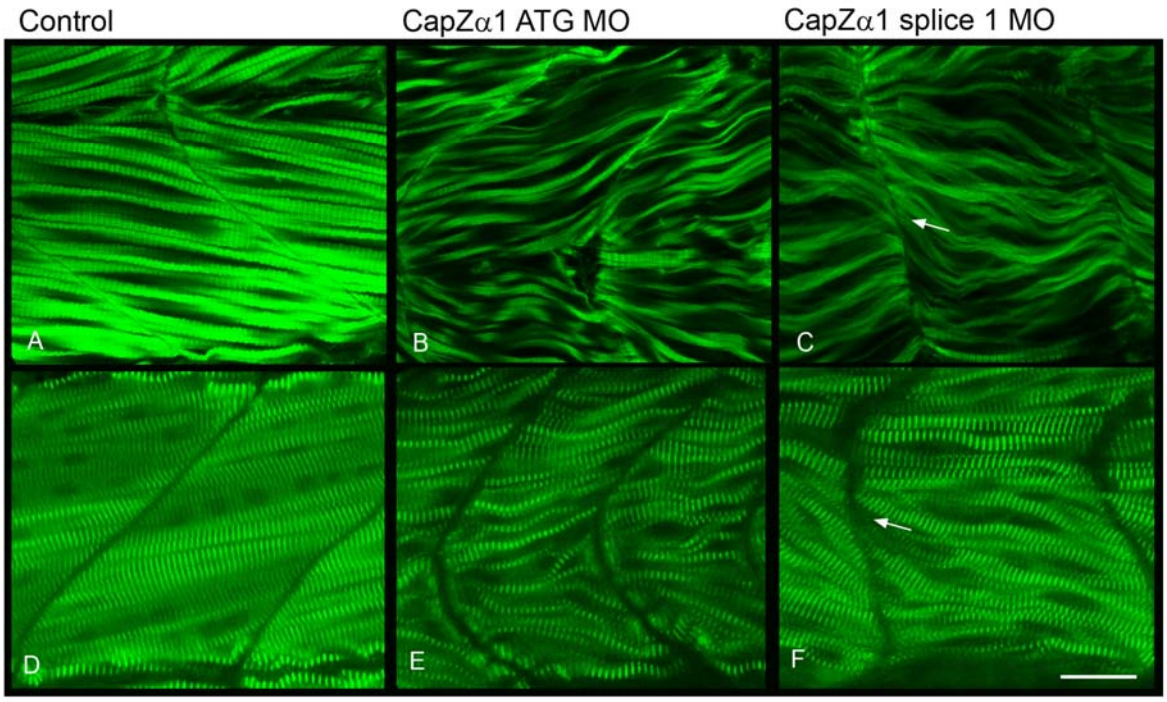

Fig. 5.3. Phalloidin and α-actinin immunostaining of 48 hpf embryos injected with capZα1 ATG and splice 1 MO. A-C) Phalloidin staining, D-F) α-actinin staining. A and D) Buffer injected control, B and E) 5ng of capZα1 ATG MO, C and F) 4ng of capZα1 splice 1 MO. Arrows in C and F indicate the U-shaped myoseptum. Scale bar = 22.18μm.

pigment, and shorter axes compared to buffer injected control embryos by 48 hpf (Fig. 5.2A and B). The somites and notochord had formed, however, the morphants were much slower to respond when prodded. The capZα1 splice 1 MO (4ng, targeted against the exon 1 donor splice site) produced a similar phenotype to the ATG MO. The splice morphants also had smaller brains and eyes, less pigment and shorter axes at 48 hpf, however, their tails were substantially more curved than the ATG morphants. Moreover, the splice morphants had acquired heart edemas (Fig. 5.2C).

Closer inspection of the skeletal muscle by phalloidin staining revealed that although F-actin had assembled within the myofibres, the filaments were wavy in both ATG and splice 1 morphants compared to the buffer injected controls at 48 hpf (Fig. 5.3A-C). The myosepta of the capZα1 splice 1 morphants also appeared u-shaped compared to the ATG morphants or the controls. α-Actinin antibody staining on both these morphants indicated that Z-lines had formed and α-actinin had localized correctly to the Z-line (Fig. 5.3D-F). This staining pattern also highlighted the presence of wavy myofibres in the morphants.

By day 5 the capZα1 splice 1 morphants were more severely affected compared to the ATG morphants. The splice 1 morphants were immotile and severely truncated with curved tails, very small brains and large heart edemas. Conversely, the ATG morphants had recovered from the effects of the MO and were comparable to controls, however, their swim bladders had not inflated and they did not respond as quickly to touch (Fig. 5.4). Phalloidin and α-actinin antibody staining of the skeletal muscle at this stage indicated that the wavy myofibres were still present. Interestingly, unlike the *sne* mutants, accumulations of mis-localized α-actinin were not observed at the myosepta (Fig. 5.5).

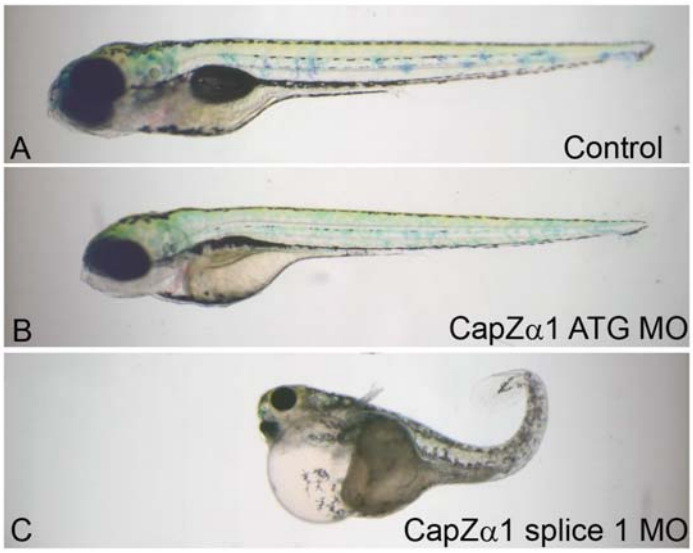

Fig. 5.4. Live images of 5 dpf embryos injected with capZα1 ATG and splice 1 MO. A) Buffer injected control, B) 5ng of capZα1 ATG MO, C) 4ng of capZα1 splice 1 MO.

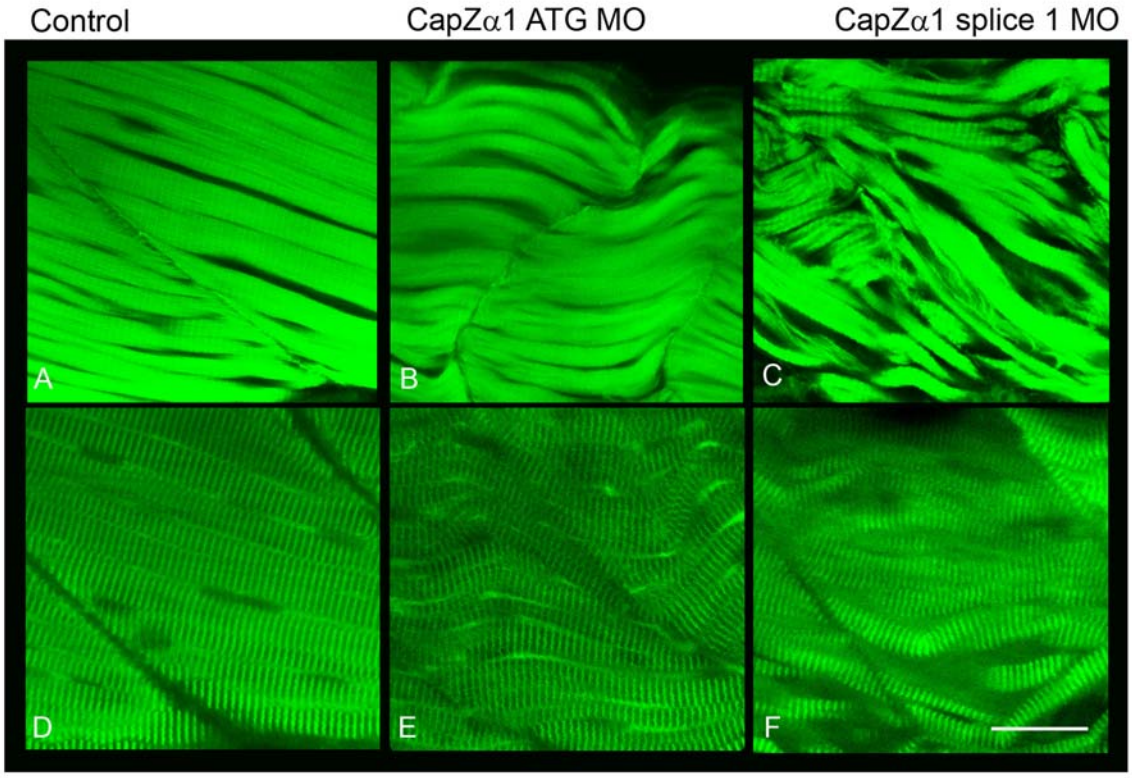

Fig. 5.5. Phalloidin and α-actinin staining of 5 dpf embryos injected with capZα1 ATG and splice 1 MO. A-C) Phalloidin staining, D-F) α-actinin staining. A and D) Buffer injected control, B and E) 5ng of capZα1 ATG MO, C and F) 4ng of capZα1 splice 1 MO. Scale bar = 22.18 μm.

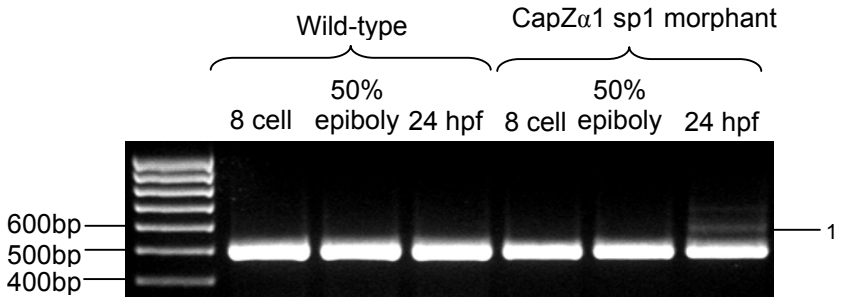

A

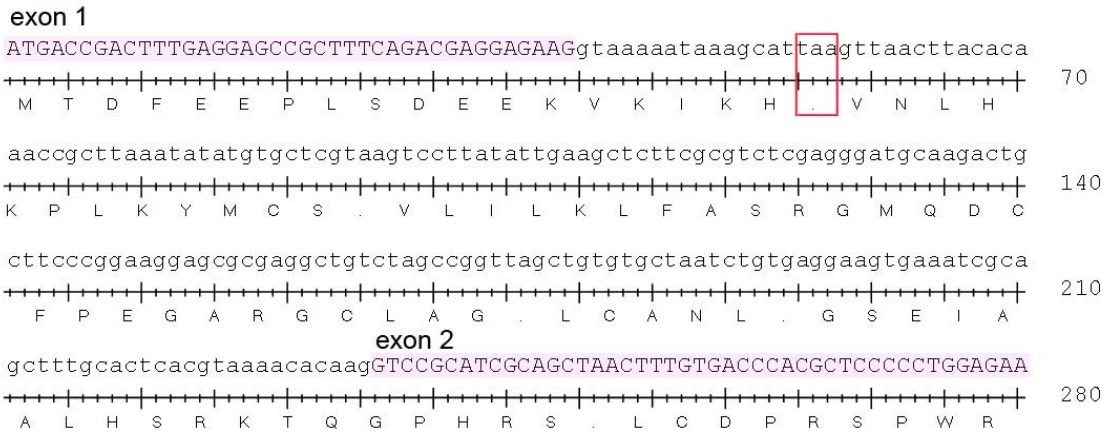

B

Fig. 5.6.A) Gel of *capzα1* RT-PCR products from cDNA of capZα1 splice 1 morphants taken at 8 cell, 50% epiboly and 24 hpf. The aberrant splice transcript (1) was observed in the 24 hpf sample only. B) DNA sequence and predicted translated protein product of the aberrant transcript cloned from the RT-PCR product (1) shown in A. The capZα1 splice 1 MO induces a mis-splicing event to occur within intron 1 and therefore the resulting protein product encodes a stop after 18 amino acids (indicated by the red box).

To verify the effectiveness of the capZα1 splice 1 MO, RT-PCR on RNA extracted from splice 1 morphants at different stages was performed, and confirmed that the splice 1 MO produces an aberrant splice transcript (Fig. 5.6A). Sequencing of this product revealed that the MO blocked splicing at the exon 1 donor splice site and induced splicing at an alternative splice site within intron 1, therefore resulting in aberrant transcription of 196bp of the intron (Fig. 5.6B). The predicted protein product from this transcript contains a termination codon 4 amino acids after translation of the transcribed intronic region, producing a truncated product of 18 aa that is unlikely to be functional.

To precisely replicate the effect of the mutation in the *sne* mutant a capZα1 splice 2 MO was designed to target the exon 9 donor splice site. Injection of 10ng of this MO produced morphants with a very similar phenotype to the *sne* mutant. On day 2, embryos appeared grossly normal compared to buffer injected controls, however, phalloidin and α-actinin staining of skeletal muscle tissue revealed that the myofibres were wavy (Fig. 5.7). At 5 dpf a similar phenotype was observed, where the MO injected embryos appeared grossly normal compared to buffer injected controls, however, lacked a swim bladder. The wavy actin filaments were also apparent by phalloidin and α-actinin staining (Fig. 5.8). Moreover, although α-actinin had localized to the Z-lines, it had also accumulated in large clumps adjacent to the myoseptum in the capZα1 splice 2 morphants.

RT-PCR was performed on cDNA from capZα1 splice 2 morphants to confirm that the MO blocked splicing at the exon 9 donor splice site (Fig. 5.9). Sequencing of the cloned RT-PCR products identified that two out of the three mis-spliced transcript isoforms expressed in the mutant were also observed in the capZα1 splice 2 morphant; the deletion of exon 9 and the addition of 46bp of intron 9. The capZα1 splice 2 morphant phenotype and the RT-PCR results

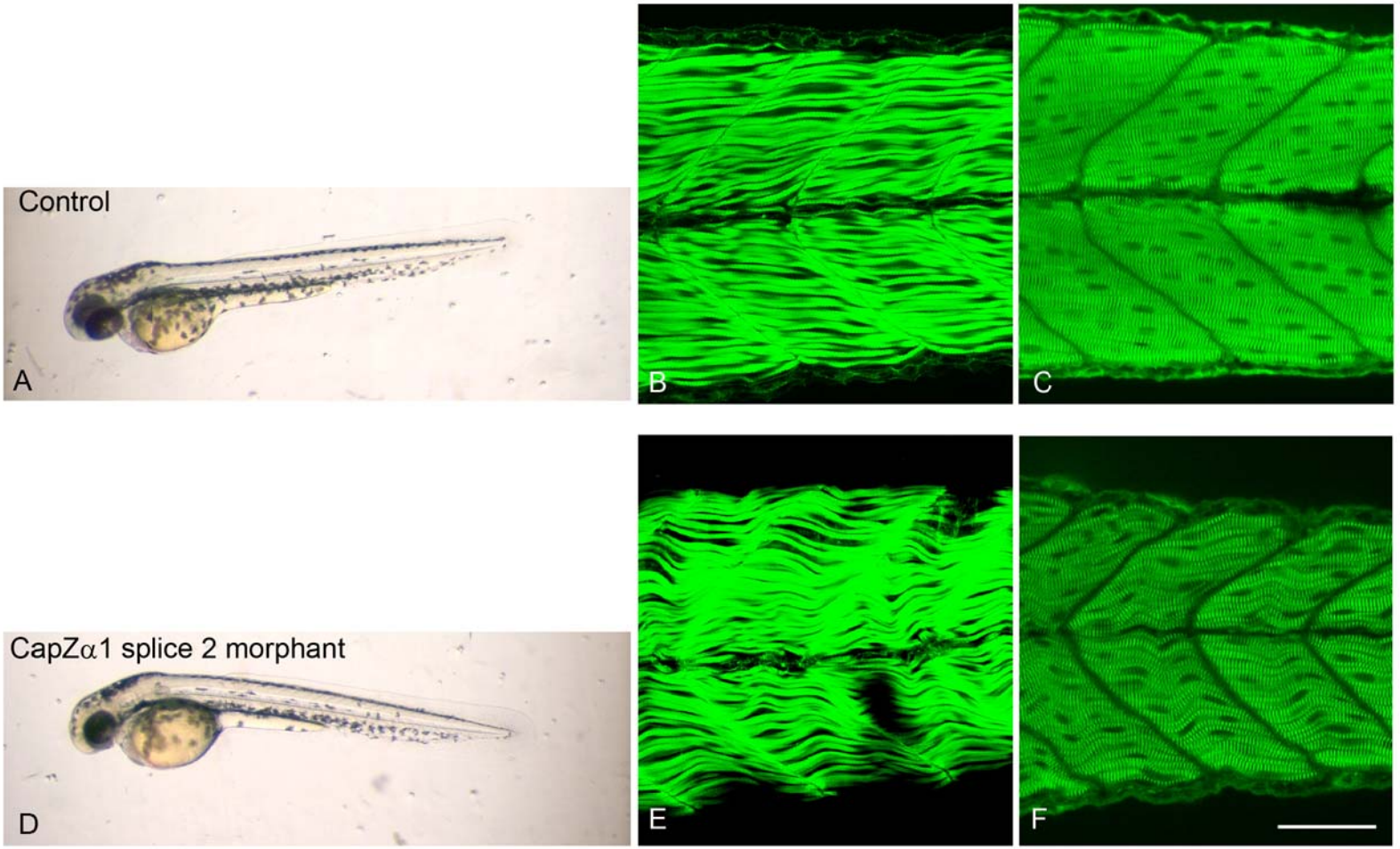

Fig. 5.7. Morphology of 2 dpf capZα1 splice 2 morphants. A-C) Buffer injected control, D-F) 10ng of capZα1 splice 2 MO, A and D) live images, B and E) phalloidin staining, C and F) α-actinin staining. Scale bar = 44.36 μm.

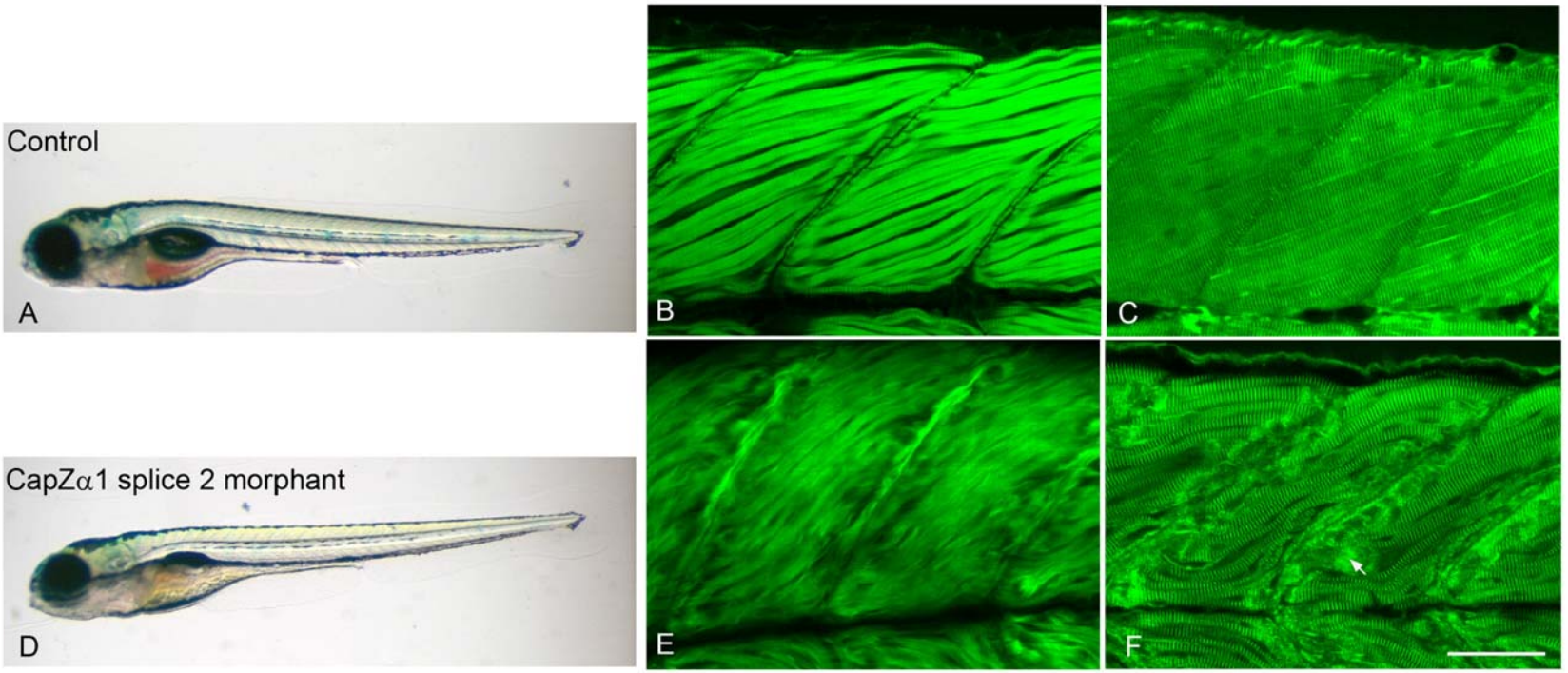

Fig. 5.8. Morphology of a 5 dpf capZα1 splice 2 morphant. A-C) Buffer injected control, D-F) 10ng of capZα1 splice 2 MO, A and D) live images, B and E) phalloidin staining, Cand F) α-actinin staining. Scale bar = 44.36μm. Arrow in F indicates the ectopic accumulation of α-actinin adjacent to the myoseptum.

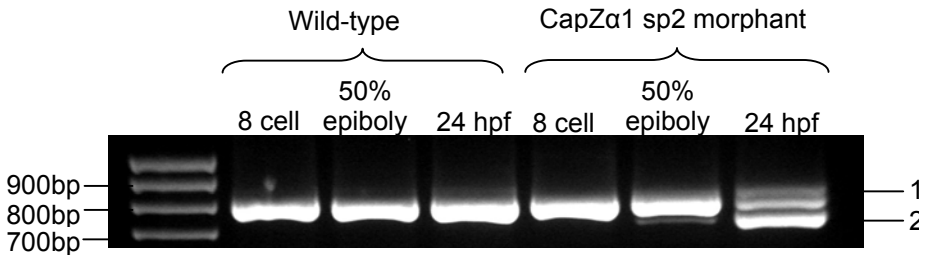

Fig. 5.9. Gel of *capzα1* RT-PCR products from cDNA of capZα1 splice 2 morphants taken at 8 cell, 50% epiboly and 24 hpf. The aberrant splice transcripts were observed in the 50% epiboly (2) and 24 hpf samples (1 and 2).

therefore confirmed that the mutation at the exon 9 donor splice site does indeed produce the *sne* mutant phenotype.

To confirm that the CapZα1 ATG and splice 1 MOs were effective in dramatically reducing CapZα1 protein levels, and also that the splice 2 MO would induce mis-localization of CapZα1, CapZα1 antibody staining on all morphants was performed. At 5 dpf there was a reduction in the localization of CapZα1 at the Z-line in all morphants (Fig. 5.10). Accumulation of CapZα1 at the myosepta was particularly prevalent in the splice 2 morphants. Unfortunately, CapZα1 antibody staining was not successful at earlier stages, therefore I was unable to observe the full effect of the MOs on CapZα1 expression and localization earlier in development. By day 5 MOs tend to be less effective, and as a result normal localization of CapZα1 was observed at the Z-line in some myofibrils of the morphants. Moreover, as the CapZα1 antibody is polyclonal, very high background levels were detected, making confocal imaging and interpreting the levels of protein difficult. Nevertheless, staining of the morphants at this stage provided circumstantial evidence that the MOs used were effective at reducing the levels of CapZα1.

Knockdown of CapZα1 using different MOs has provided some preliminary clues as to the nature of the *sne* phenotype. It was speculated that the *sne* mutant may have a milder phenotype due to the maternal contribution of CapZ, however, this is clearly not the case as the early splice MO (splice 1, which does not knockdown the maternal contribution) gives the same phenotype as the ATG MO (which knockdowns maternal contribution). As the early splice morphant also produces a more severe phenotype than late splice (splice 2), this also indicates that the aberrant protein product that is produced in the mutant and has some partial function.

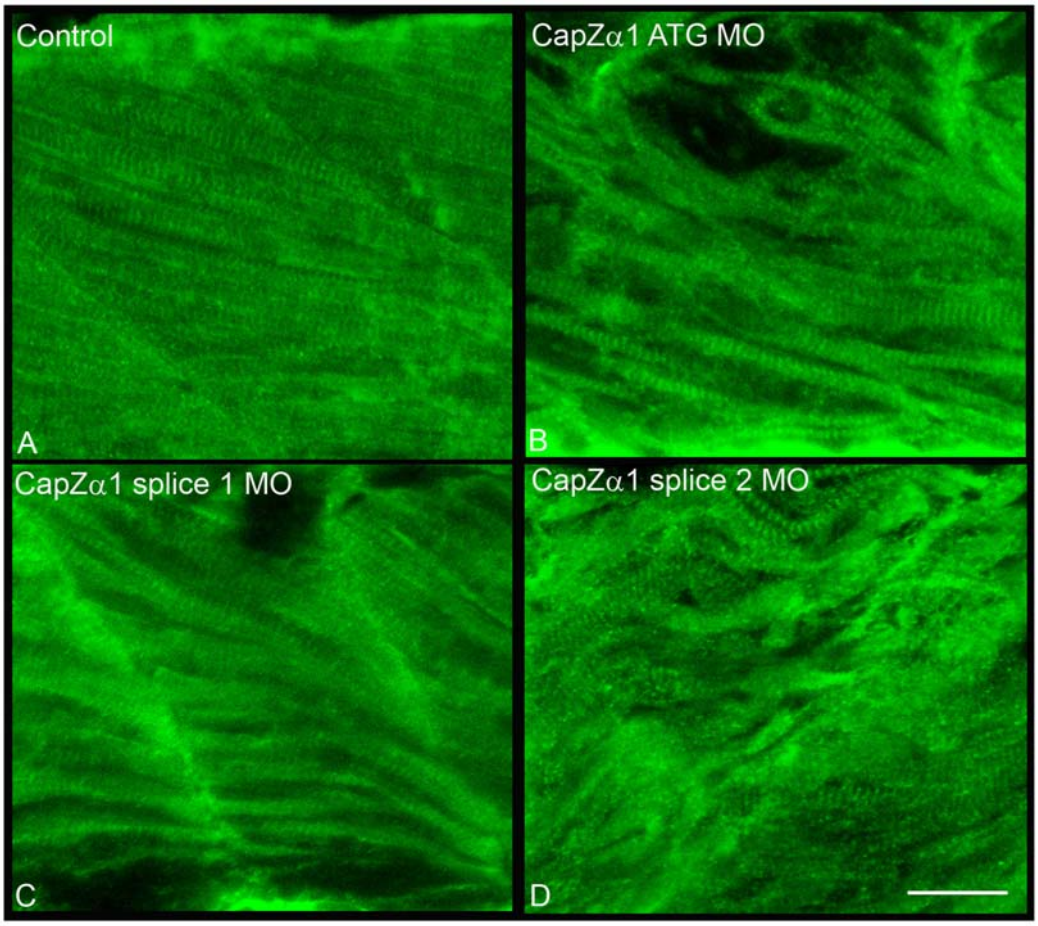

Fig. 5.10. CapZα1 antibody staining of capZα1 morphants at 5 dpf. A) Buffer injected control, B) 5ng of capZα1 ATG MO, C) 4ng of capZα1 splice 1 MO, D)10ng of capZα1 splice 2 MO. Scale bar = 22.18μm.

5.3.2 MO knockdown of CapZα2

To determine whether CapZα2 also plays a role in compensating for a lack of completely functional CapZα1 in the *sne* mutant, an ATG and splice MO were designed to knockdown the α2 subunit. Intriguingly, the capZα2 ATG and splice MOs produced quite variable phenotypes. Injection of only 1.5ng of the capZα2 ATG MO caused severe developmental defects. By 24 hpf the embryos were severely delayed and had a smaller brain and eyes, as well as u-shaped somites, however, side to side movement of the tail was still observed. By 48 hpf the ATG morphants had a shortened axes, smaller brains, curved tails, heart edemas and less pigment compared to controls (Fig. 5.11A and C), and by day 5 most of the morphants had not survived. Unexpectedly, injection of 6ng of the capZα2 splice MO did not affect the morphology of injected embryos. At 48 hpf they swam normally and had very straight axes, although their brains were slightly smaller and reduced pigmentation levels were observed compared to controls (Fig. 5.11B). On day 5 the splice morphants still had a similar morphology to buffer injected embryos (Fig. 5.11D and E).

Phalloidin and α-actinin staining of these morphants revealed that actin filaments and Z-lines had formed in the ATG morphant, however, the actin filaments were not as straight as the wt equivalents on day 2 (Fig 5.12C and F). As expected from its gross morphology, the staining pattern of the splice morphant was indistinguishable from the wt on both day 2 (Fig. 5.12B and E) and day 5 (Fig. 5.13A-D). CapZα1 antibody staining also indicated that CapZα1 was normally localized to the Z-line on day 5 in the splice morphant (Fig. 5.13E and F).

5.3.2.1 The CapZα2 ATG MO knocks down CapZα1

The capZα2 ATG MO sequence only differs by 4bp to the coding region surrounding the ATG of *capzα1*. According to the MO manufacturer this difference should be sufficient to ensure

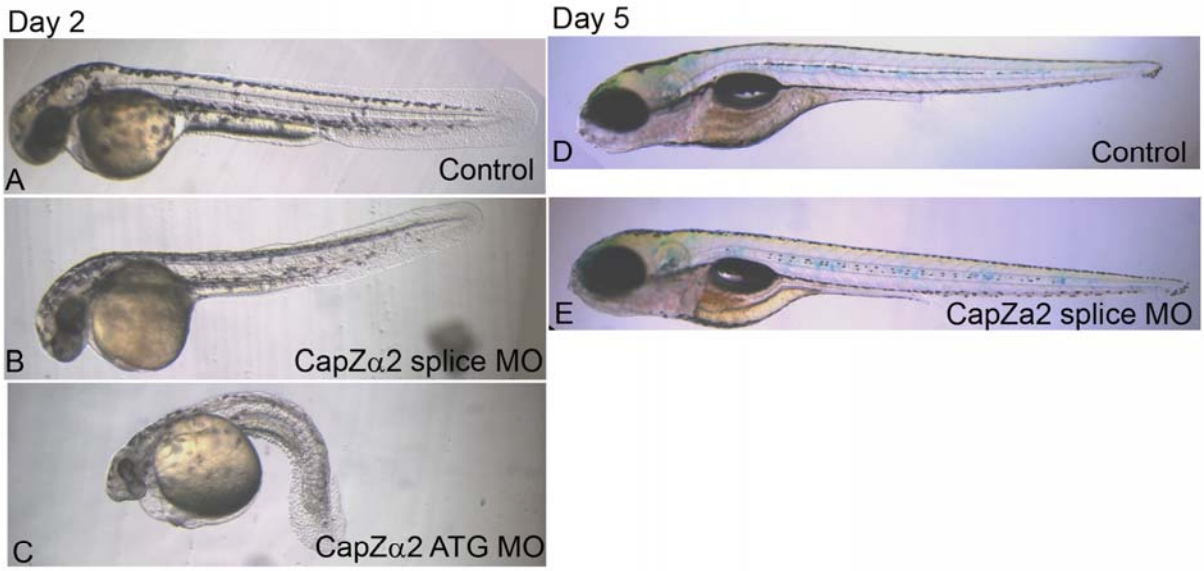

Fig. 5.11. Day 2 (A-C) and day 5 (D-E) live images of capZα2 ATG and splice morphants. A and D) buffer injected control, B and E) 6ng of capZα2 splice MO and C) 1.5ng of capZα2 ATG MO.

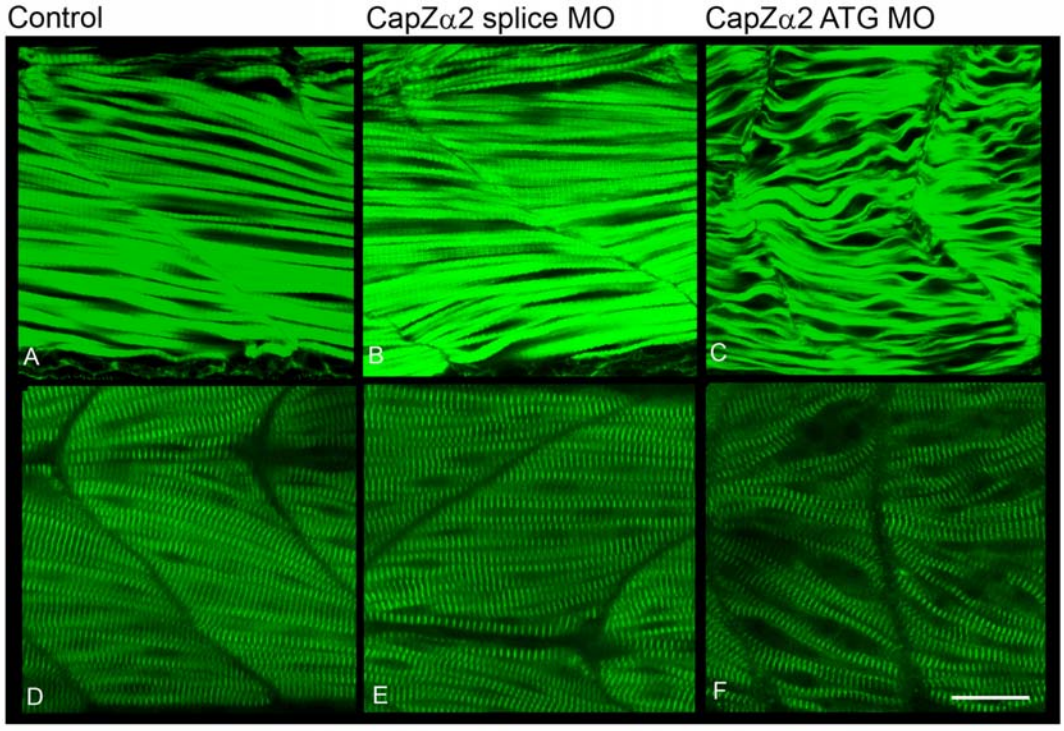

Fig. 5.12. Phalloidin (A-C) and α-actinin staining (D-F) of day 2 capZα2 ATG and splice morphants. A and D) buffer injected control, B and E) 6ng of capZα2 splice MO, C and F) 1.5ng of capZα2 ATG morphant. Scale bar = 22.18 μm

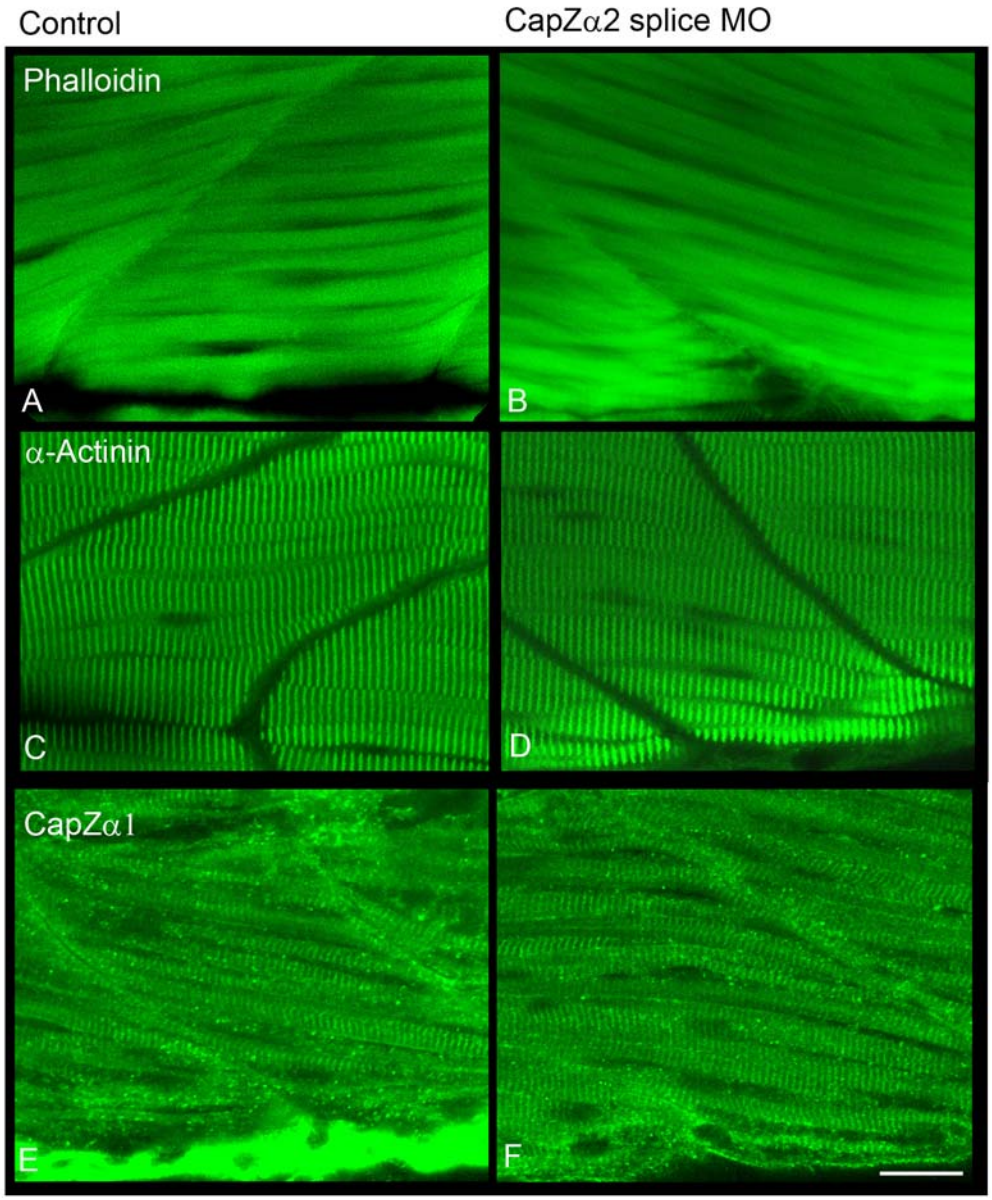

Fig. 5.13. Phalloidin A and B), α-actinin C and D) and CapZα1 staining E and F) on 5 dpf capZα2 splice morphants.A, C and E) buffer injected control, B, D and F) 6ng of capZα2 splice MO. Scale bar = 22.18 μm.

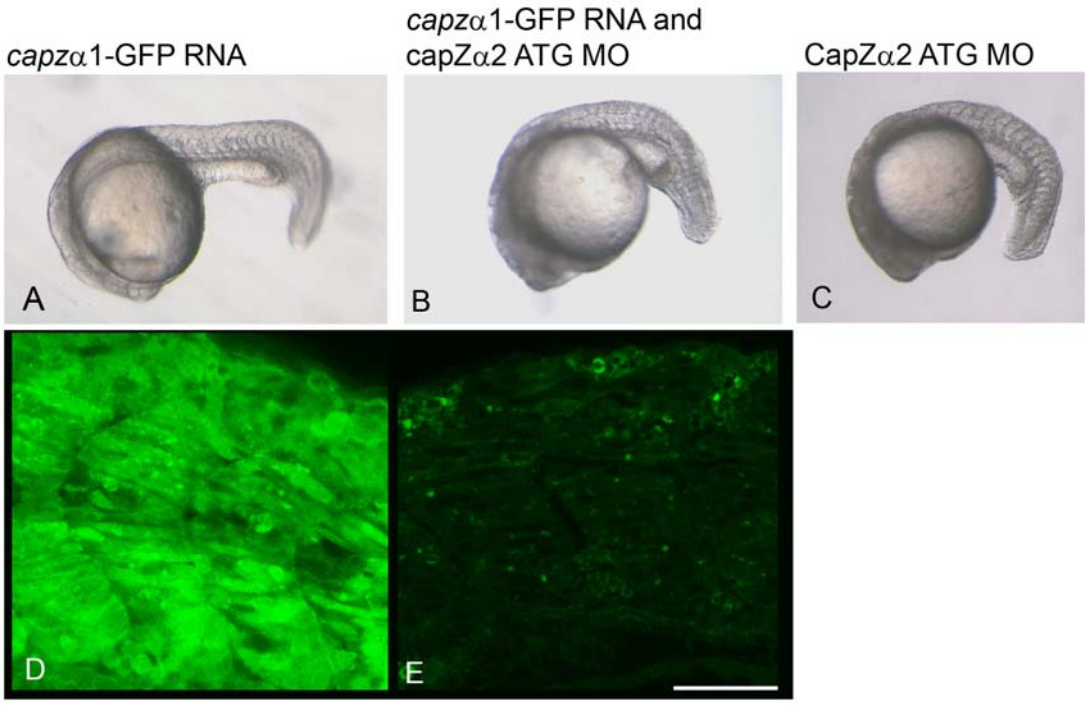

Fig. 5.14. Twenty hpf embryos that were co-injected with *capzα1*-GFP RNA and capZα2 splice MO at the 1-2 cell stage. A, B and C) live images, D and E) confocal images of embryos expressing CapZα1-GFP. A and D) Embryo injected with 150pg of *capzα1*-GFP RNA only, B and E) embryo injected with 150pg of *capzα1*-GFP RNA and 1.5ng of capZα2 ATG MO. C) Embryo injected with 1.5ng of capZα2 ATG MO only. Scale bar = 44.36 μm.

that the MO binds to a specific site. However, due to the severity of the capZα2 ATG morphant, I suspected that this MO was able to bind to the start site of both *capzα1* and *capzα2* RNA and block translation. To test this hypothesis, I co-injected *capzα1*-GFP RNA (150pg) (described in further detail in section 5.4) and capZα2 ATG MO (1.5ng) into 1-2 cell stage embryos, and after 20 hpf observed the GFP expression. Confocal imaging of the co-injected embryos indicated that addition of capZα2 MO severely reduced the translation of CapZα1-GFP (Fig. 5.14), and therefore demonstrates that the capZα2 ATG MO is also able to knockdown CapZα1.

5.3.3 MO knockdown of CapZβ

Two isoforms of *capzβ* are expressed in all tissues of higher vertebrates and are transcribed from one gene. Unfortunately, I was only able to detect the *capzβ2* isoform in zebrafish, however, it seems likely that two isoforms also exist in this species. Presuming that a *capzβ1* and *capzβ2* isoform are expressed in zebrafish, both the ATG and splice MOs designed against this gene should target each isoform, which only differ in their C-terminal region. Injection of 6ng of ATG MO did not affect the outward appearance of the injected embryo on day 2 (Fig. 5.15), however, injection of 3ng of the splice MO produced embryos with smaller brains, shorter axes, and fewer pigmented cells than the wt controls. Both the ATG and the splice morphants reassuringly produced a similar muscle phenotype to the capZα1 morphants at 48 hpf. Phalloidin and α-actinin staining at this stage revealed that in both morphants actin filaments and Z-lines had formed and the myofibrils were wavy, however, the ATG morphant myofibrils were not as wavy as the splice morphant (Fig. 5.16).

On day 5 the jaw of the splice morphants had not formed properly and the swim bladder had not inflated, but embryos moved normally (Fig. 5.17). The ATG morphants also had a

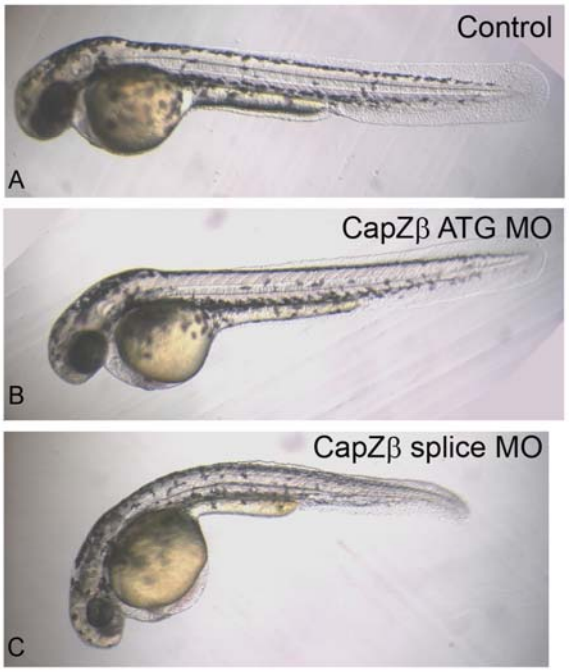

Fig. 5.15. CapZβ ATG and splice morphants at 2 dpf. A) Buffer injected control, B) 6ng of capZβ ATG MO, C) 3ng of capZβ splice MO.

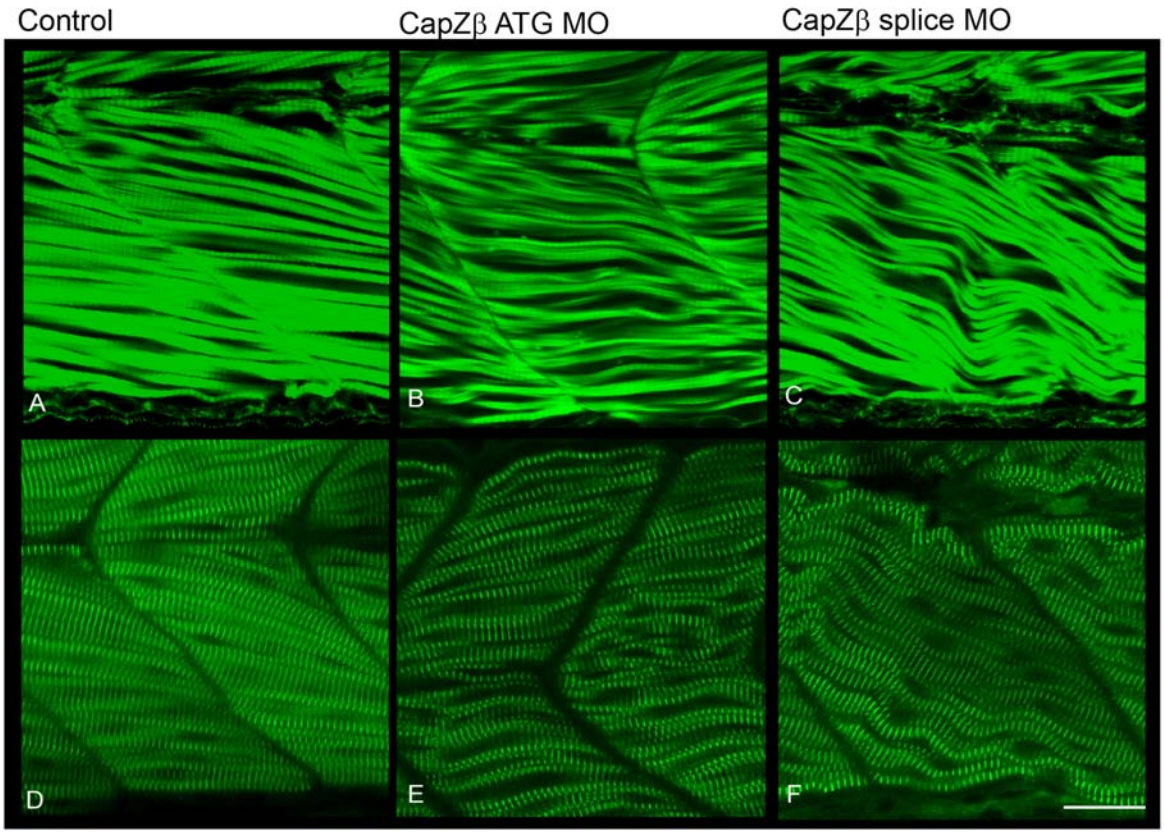

Fig. 5.16. Phalloidin (A-C) and α-actinin staining (D-F) of capZβ ATG and splice morphants at 2 dpf. A and D) Buffer injected control, B and E) 6ng of capZβ ATG MO, C and F) 3ng of capZβ splice MO. Scale bar = 22.18 μm.

deformed jaw and uninflated swim bladder. Additionally, the edges of both the dorsal and ventral fins were ragged (Fig. 5.17B arrow), which was not observed in the splice morphants. Interestingly, the ragged fin phenotype has previously been observed in a retroviral insertional *capzβ* mutant (capzβ^{hi1858bTg}) by Amsterdam et al., 2003 (Fig. 5.17D). The phalloidin and α-actinin staining pattern of the morphants on day 5 was very similar to day 2, however, the ATG morphants had much wavier myofibrils at this stage (Fig. 5.18A-F). Intriguingly, accumulations of mis-localized α-actinin at the myosepta were detected in the splice morphants and resembled the *sne* mutant phenotype.

CapZα1 antibody staining of the CapZβ ATG and splice morphants on day 5 revealed that CapZα1 was not localized to Z-line in either of the morphants and had accumulated at the myosepta (Fig. 5.18G-I). In addition to the accumulation of α-actinin at the myosepta and the wavy myofibrils, this result indicates that in the absence of CapZβ, CapZα1 is unable to localize to the Z-line. As the loss of CapZβ partially phenocopies the morphology of the *sne* mutant, it could be proposed that in the mutant, defective CapZα1 is unable to bind to CapZβ and therefore becomes mis-localized.

Higher doses of capZβ MO did induce a more severe phenotype that was similar to the double knockdown of the α subunits using the capZα2 ATG MO. Injection of 8ng of capZβ ATG MO produced embryos that were developmentally delayed with gross morphological defects. By day 5 both the capZβ and capZα2 ATG morphants suffered from heart edemas, severely truncated axes, small brains and eyes, and were immotile (Fig. 5.19). These phenotypes confirm that CapZ is non-functional if either α or β subunits are lost.

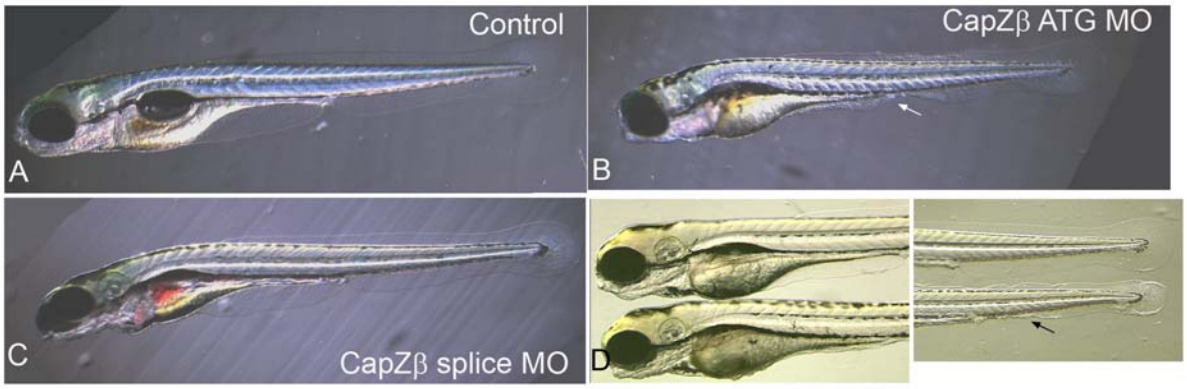

Fig. 5.17. CapZβ ATG and splice morphants at 5 dpf. A) Buffer injected control, B) 6ng of capZβ ATG MO, C) 3ng of capZβ splice MO, D) 5 dpf *capz*β retroviral mutant generated in Nancy Hopkins laboratory (image taken from Amsterdam et al., 2003). The embryo on top is wild-type and on the bottom is a mutant. Note the frayed ventral fins in the ATG morphant and the retroviral mutant (arrows).

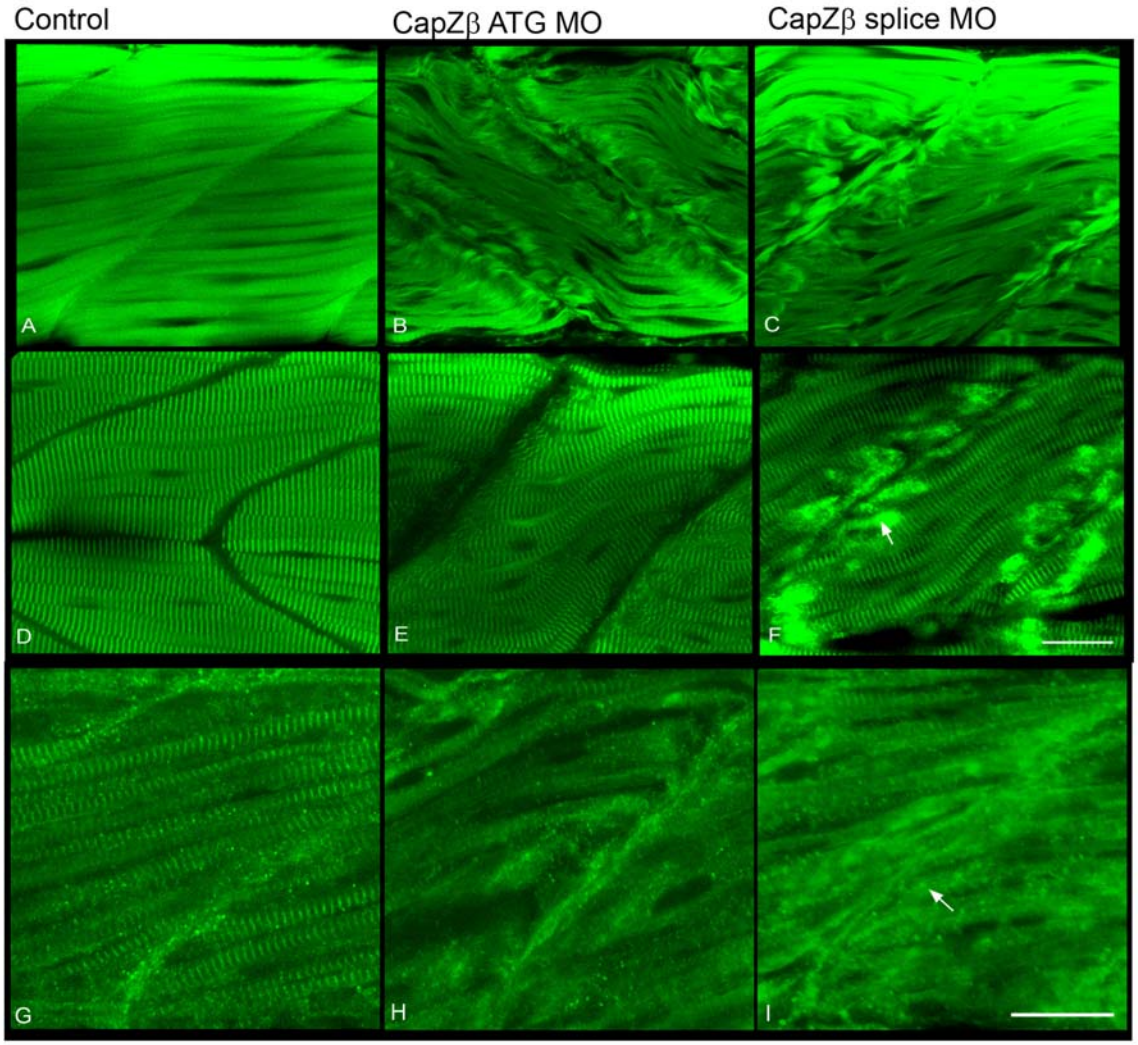

Fig. 5.18. Phalloidin (A-C), α-actinin (D-F) and CapZα1 staining (G-I) of capZβ ATG and splice morphants at 5 dpf. A, D and G) Buffer injected control, B, E and H) 6ng of capZβ ATG MO, C, F and I) 3ng of capZβ splice MO. Scale bar = 22.18 μm for images A-F and G-I.Arrows in F and I indicate accumulations of α-actinin and CapZα1 respectively.

Fig. 5.19. Live images at 5 dpf of A) a capZα2 ATG morphant (1.5ng) and B) a capZβ ATG morphant (8ng).

5.3.4 Detection of CapZα1 in mutant and morphants by Western blotting

Western blotting was performed to conclusively determine if any CapZα1 was translated in the mutant, and as an additional measure to determine the effectiveness of the MOs. As the chicken polyclonal CapZα1 antibody used in whole mount staining was not specific in the Western, a monoclonal IgG mouse CapZα antibody (BD Life sciences), targeted against the N-terminal region (1-108 amino acids) of human CapZα was used. Using this monoclonal antibody I was able to detect a single band from wild type and mutant protein extracts (Fig. 5.20A), however, the band was not of the expected size (should be ~37 kDa). It is possible that this size discrepancy is due to differences in post translational modifications between species.

Due to the similarity of CapZα1 with CapZα2 it was speculated that the antibody is able to bind to both subunits. However, as both α isoforms are of a similar size (32.73 and 32.77kDa respectively) it is unlikely that I would be able to discern differences in CapZα1 levels in a Western from a one dimensional gel. I therefore repeated the Western on protein extracted from embryos injected with either the capZα1 and/or capZα2 ATG MO: Firstly, to decipher whether the antibody bound to both α subunits and secondly, to confirm that the antibody did indeed bind to CapZ subunits. If the antibody recognized both α subunits, I would expect a reduction in the band intensity of the embryos co-injected with capZα1 and capZα2 MO. If the antibody only bound to capZα1 then there should be a reduction in the band intensity of protein extracted from the capZα1 MO injected embryo and the double knockdown. Unfortunately, no discernable differences in the levels of the band intensity were detected (Fig. 5.20B). This suggests that this antibody is not binding to CapZα at all. An alternative explanation is that as the embryos were taken at shield stage, excess maternal protein is detected and is masking the knockdown effect of

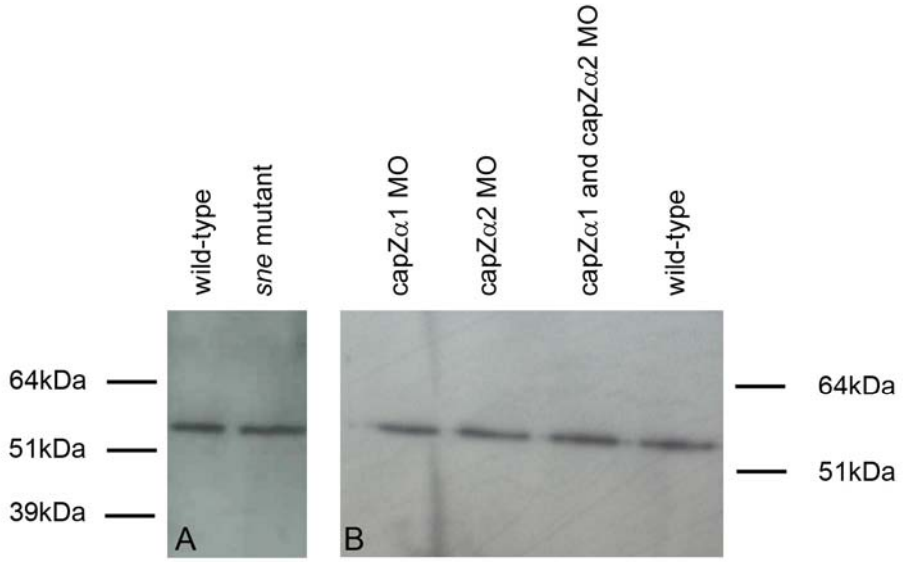

Fig. 5.20. Western blots on protein isolated from *sne* mutant and capZ morphants using the mouse monoclonal CapZα antibody. A) Western blot using wild-type protein extracted from 24 hpf embryos. Mutant protein was isolated from a 5 dpf indivudual *sne* mutant embryo. B) Western blot using equivalent amounts of protein extracted from 50% epiboly stage embryos injected with capZα1 MO (8ng),capZα2 MO (6ng), co- injected with capZα1 MO (8ng) and capZα2 MO (6ng), and wild-type controls.

the MOs. Therefore, using this approach I was not able conclusively establish whether any CapZα1 was produced in mutants.

5.4 Rescue of the capZα1 morphant using *capzα1*-GFP RNA

To confirm the localization of CapZα1 within the muscle and to determine whether exogenous CapZα1 could rescue the morphant phenotype, a CapZα1-GFP construct was generated. The GFP sequence was ligated to the 3′ end of *capzα1* via an 18bp linker, to ensure the GFP was able to fold correctly once translated. The whole construct was ligated into a pCS2+ vector and the capped RNA transcribed *in vitro* using an SP6 polymerase. Injection of up to 200pg of *capzα1*-GFP RNA had no effect on muscle development or the morphology of the muscle, and *capzα1*-GFP RNA was expressed and localized to the Z-line and myoseptum (as confirmed by double staining with α-actinin) (Fig. 5.22B-D). This finding supports the CapZα1 antibody staining pattern and verified that CapZα1-GFP can still dimerize with the β subunit to form functional CapZ.

capzα1-GFP RNA (150ng) was co-injected into 1-2 cell stage embryos with 4ng of capZα1 ATG MO, to determine whether exogenous CapZα1 could rescue the morphant phenotype. The ATG MO was used rather than splice 2 MO or the *sne* mutant because the defect is seen much earlier and therefore any amelioration of the phenotype would be much easier to score. By 48 hpf rescued embryos looked slightly better than MO only injected embryos. Although they had a smaller axes and brains in addition to reduced pigment, there was slightly more pigment in the RNA and MO injected embryos than in MO only injected embryos (Fig. 5.21). The skeletal muscle was then stained with α-actinin and the myofibrillar structure examined. Rescued embryos had straighter myofibrils than those embryos that were not injected

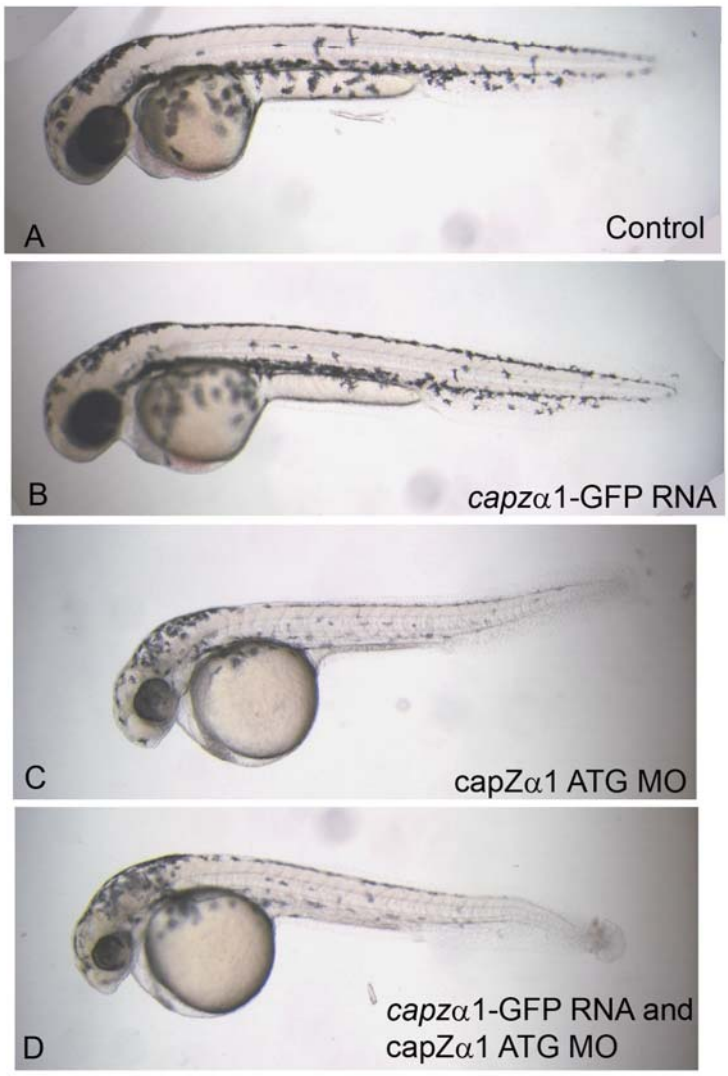

Fig. 5.21. Live images of embryos co-injected with capZα1 ATG MO and *capzα1*-GFP RNA. A) Buffer injected control, B) 150pg of *capzα1*-GFP RNA only, C) 4ng of capZα1 ATG MO only and D)150pg of *capzα1*-GFP RNA and 4ng of capZα1 ATG MO.

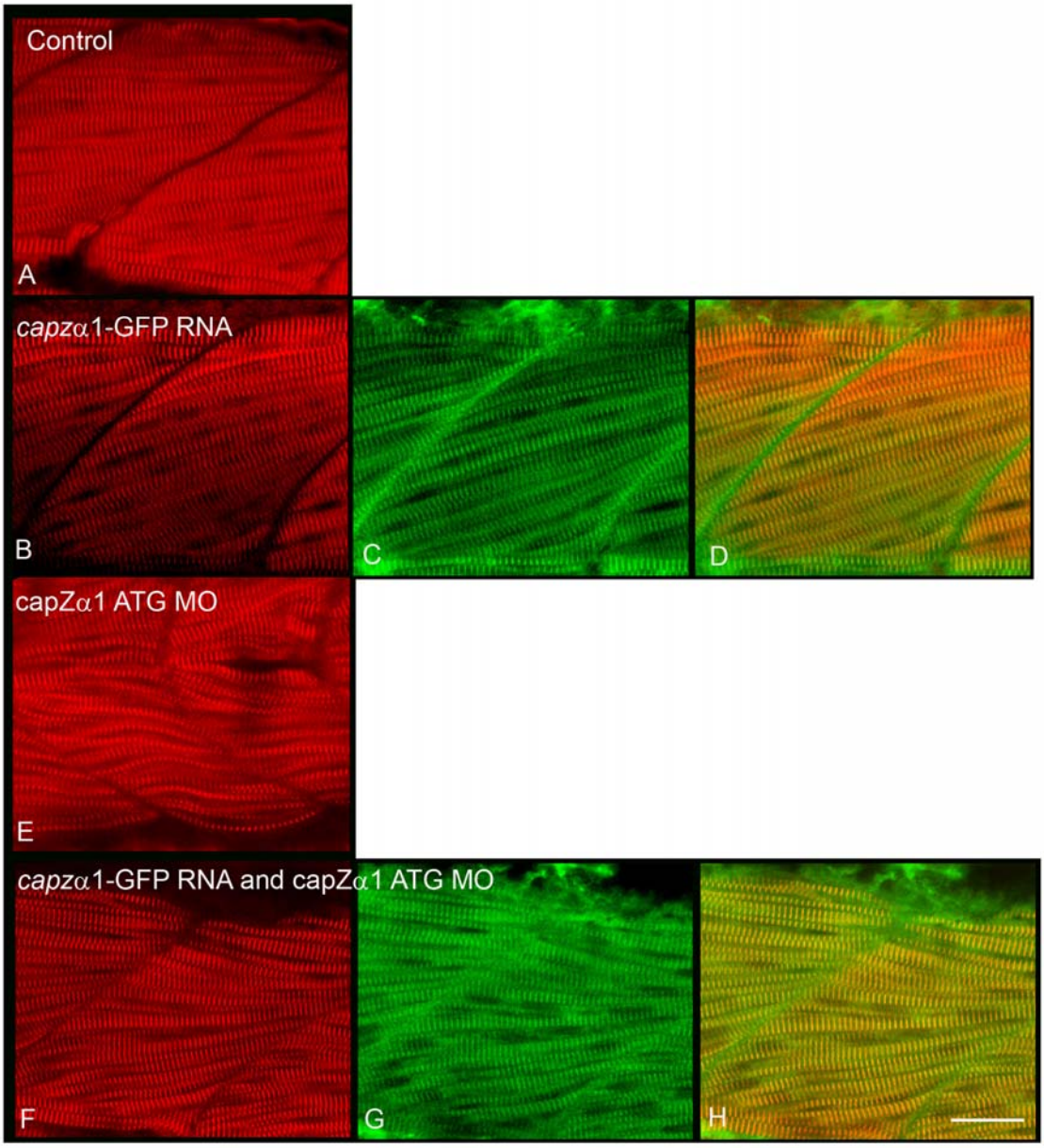

Fig. 5.22. Skeletal muscle confocal images of capZα1 ATG morphants rescued with *capzα1*-GFP RNA. A, B, E and H) α-Actinin staining (red), C and G) CapZα1-GFP expression (green), and D and H) merge of α-actinin and CapZα1-GFP images. A) Buffer injected control, B-D)150pg of *capzα1*-GFP RNA only, E) 4ng of capZα1 ATG MO only and F-H) 150pg of *capzα1*-GFP RNA and 4ng of capZα1 ATG MO. Scale bar = 22.18 μm.

with *capzα1*GFP RNA, and CapZα1-GFP had incorporated into the Z-lines and the myoseptum (Fig.5.22).

5.5 Discussion

The use of an ATG and two different splice MOs to knockdown CapZα1 has shed new light on the nature of the *sne* mutant and the role of CapZα1 in other aspects of embryonic development. Firstly, the *sne* mutant could be phenocopied by injecting embryos with a MO (splice 2) designed against the exon 9 donor splice site of *capzα1*. This strongly confirmed the site of the mutation in the *sne* mutant. Moreover, co-injection of *capzα1*-GFP RNA with the capZα1 ATG MO partially rescued the capZα1 ATG morphant phenotype. Secondly, injection of the ATG or splice 1 MO (which targets the exon 1 donor splice site) produced a more severe phenotype than the mutant or the splice 2 morphant. This indicated that the CapZα1 mis-spliced products present in the capZα1 splice 2 morphant (and therefore the *sne* mutant) must be partially functional. However, as all three morphants displayed wavy skeletal muscle fibres, this suggests that CapZα1 function in the muscle is severely affected in all capZα1 morphants. Indeed, CapZα1 antibody staining on day 5, suggests that in all three capZα1 morphants, CapZα1 is non-functional in skeletal muscle, either as a result of complete depletion of the protein or mis-localization. In this respect all morphants replicated the *sne* mutant phenotype.

The maternal contribution of *capzα1* could be an important factor in reducing the severity of the *sne* mutant phenotype compared to the ATG morphant. However, the splice 1 morphant has a similar phenotype to the ATG morphant suggesting that the maternal contribution has no bearing on the *sne* mutant phenotype. Rather, the more severely affected ATG and splice 1 morphants indicate that CapZα1 may be required much earlier in development. The mis-spliced

products that are translated in the *sne* mutant may be sufficient to carry out functions early in development, resulting in a milder phenotype compared to the ATG and splice 1 morphant where no CapZα1 is expressed. However, at the later stages of development, when CapZα1 is required in skeletal muscle, the mutant forms are unable to function in this tissue and the muscle specific phenotype is observed.

Knockdown of CapZα2 was also performed to determine whether CapZα2 could compensate for the loss of CapZα1. The ATG capZα2 MO produced a very severe phenotype at low doses, and co-injection with *capzα1*-GFP RNA established that this was because the ATG MO is able to knockdown expression of both the α1 and α2 transcripts. Unexpectedly, injection of the capZα2 splice MO did not produce a phenotype at all. This indicates that either the MO is not effective or the α1 subunit is able to rescue the phenotype in the absence of the α2 subunit. The latter theory is plausible as the RNA *in situ* hybridization expression patterns (shown in chapter 4) revealed that at 24 hpf there were higher levels of *capZα1* expression compared to *capZα2* in the muscle. However, further analysis is required to establish whether the CapZα2 splice MO is actually knocking down CapZα2.

In higher vertebrates the *capzβ1* and *capzβ2* isoforms are transcribed from one gene and only differ in their C-terminal regions. In zebrafish only one isoform has been identified, however, MOs against CapZβ were designed to knockdown both isoforms (if they do indeed exist). Functional CapZ requires the dimerization of α and β subunits, therefore loss of CapZβ would be predicted to produce a similar phenotype to the loss of the α subunits. As expected, both the capZβ ATG and splice MO produced a similar wavy myofibre phenotype to the capZα1 morphants, however, the ATG morphant phenotype was not as severe as the splice morphant. Generally, an ATG MO will produce a more severe phenotype than the splice as it knocks down

the maternal transcript as well as the embryonic transcript, which starts to be expressed at around the 1000 cell stage. It is possible that in this case the splice MO may be more efficient at knocking down the CapZβ subunit and therefore produce a more severe overall phenotype than the ATG MO. In any case RT-PCR experiments on capZβ splice morphants at different stages are required to confirm that the splice MO is knocking down translation of the transcript. However, due to the very specific phenotype that correlates with the *sne* phenotype it is more than likely that the MO is functioning correctly.

High doses of the CapZβ ATG MO replicated the severe defects observed in the capZα2 ATG morphant (which knocks down both α subunits). These findings therefore corroborate previous studies where the loss of either the α or β subunit prevents the formation of CapZ (Amatruda et al., 1992; Hug et al., 1995; Hug et al., 1992; Schafer et al., 1992), resulting in the same phenotypic defect being observed when either subunit is depleted. However, it cannot be ruled out that these phenotypes are not due to a general toxic effect of the MO (Robu et al., 2007). Co-injection with a p53 MO may assist in proving whether this phenotype is genuine. Additional Western analysis may also be beneficial in showing the effectiveness of each MO.

Antibody staining of CapZα1 on capZβ morphants revealed that CapZα1 had accumulated at the myoseptum. This particular phenotype is identical to what is observed in the *sne* mutant and supports the hypothesis that in the mutant an aberrant form of the CapZα1 protein is produced but is unable to dimerize with the β subunit, and therefore mutant CapZα1 accumulates at the myoseptum. Conversely, in the capZβ1 morphant, as the α1 subunit is unable to dimerize to form CapZ due to a lack of the β subunit, CapZα1 aggregates are also observed adjacent to the myoseptum.

The aberrant staining pattern of mis-localized α-actinin aggregates at the myoseptum is observed in the *sne* mutant as well as in the CapZβ morphant, however, is absent in the capZα1 ATG and splice 1 morphants. The differences in α-actinin accumulation indicate that this phenomenon is an artefact of the accumulation of the unincorporated mutant form of CapZα1, which is still able to bind to α-actinin. This theory is supported by the fact that the capZβ morphant produces the same phenotype and in these embryos normal CapZα1 protein would be produced. Unusually, the accumulations were not seen earlier than day 5, which suggests that over time sarcomeric components start to disassemble from a lack of functional CapZ, and eventually accumulate ectopically. The notion that the α1 subunit alone is able to bind to α-actinin contradicts a study done by Papa and colleagues in 1999, which identified that only the CapZ heterodimer was able to bind to α-actinin. As these studies were done *in vitro* it is quite possible that *in vivo* the α1 subunit is able to bind to α-actinin. Further experiments will be required to determine conclusively whether α-actinin or CapZβ can still bind to the mis-spliced CapZα1 product produced in the mutant.

Interestingly the capZβ ATG morphant produces a slightly different gross morphology to the splice morphant. Although both morphants produce a wavy myofibre phenotype, the ATG morphant also has ragged dorsal and ventral fins that become visible by 5 dpf, which are not observed in the splice morphant. As this phenotype was also seen in the *capZβ* retroviral mutant (capZβ^{hi1858bTg}) (Amsterdam et al., 2004) it verifies that the MO is effectively knocking down *capZβ*.

The MO analysis on the different subunits of CapZ has provided further insight to the nature of the *sne* mutant. It is likely that the mutation in *sne* results in the translation of mis-spliced forms of CapZα1, which are unable to dimerize with the β subunit or localize to Z-lines,

due to an inability to bind to the β subunit. Although the whole mount antibody staining provided evidence that CapZα1 protein is expressed in the *sne* mutants, Western blotting is still necessary to determine the number, type and abundance of mis-spliced transcripts that are translated. This experiment was performed but was unsuccessful as I was unable to establish whether the antibody specifically bound to CapZα1. Specific monoclonal antibodies against the α1 and α2 subunits have been generated (Hart et al., 1997b; Schafer et al., 1996), and may be more useful in detecting the presence of any protein product in the mutant. It has also been shown that the α1 and α2 subunits can be separated on a two dimensional (2D) gel (Hart et al., 1997b). In future, Western blotting experiments should incorporate 2D gels to separate the mutant α1 subunits and they should be detected using unique antibodies. This type of experiment will be more informative in determining conclusively which forms of mis-spliced transcripts are translated. Once the predominant mis-spliced CapZα1 product has been identified it will be easier to investigate precisely how the truncated product induces the phenotype. For example, its exact location within the cells during development could be determined by generating a GFP fusion construct, and the extent of its function and binding capability with other sarcomeric proteins could also be tested.

It is clear that CapZ is involved in many aspects of cell development, not just in skeletal muscle function. The different subunits are likely to have diverse roles in the cell and may be important in early developmental processes. Further research is required to fully understand the functions of the individual subunits and how they affect the role of CapZ during development.